

## Article

# Efficient Zero-Value-Cross Detection for Single-Phase Mains-Powered Motors: A Comparative Study

Mariusz Pauluk , Paweł Piątek  and Jerzy Baranowski \* 

Faculty of Electrical Engineering, Automatics, Computer Science, and Biomedical Engineering, Department of Automatic Control and Robotics, AGH University of Krakow, al. A. Mickiewicza 30, 30-059 Krakow, Poland; mp@agh.edu.pl (M.P.); ppi@agh.edu.pl (P.P.)

\* Correspondence: jb@agh.edu.pl

**Abstract:** This paper proposes solutions for zero-value-cross detection (ZVCD) in a single-phase mains-powered motor used for high-torque tightening. Four different applications are presented: resistor-polarized digital input, a resistor-polarized optocoupler, comparators steering up the optocoupler, and n-MOSFETs polarizing the optocoupler. The performance of each solution is evaluated in terms of complexity, dimensions, power dissipation, and response time. The n-MOSFET-based solution is found to be the most suitable, providing a simple design, low power dissipation, and almost instantaneous response. This solution meets the project's requirements for accurate and fast zero-crossing detection.

**Keywords:** zero-value-cross detection; single-phase motors; power tool; high torque; n-MOSFETs; optocoupler



**Citation:** Pauluk, M.; Piątek, P.; Baranowski, J. Efficient Zero-Value-Cross Detection for Single-Phase Mains-Powered Motors: A Comparative Study. *Energies* **2023**, *16*, 6298. <https://doi.org/10.3390/en16176298>

Academic Editors: Akhtar Kalam and Seyed Morteza Alizadeh

Received: 22 July 2023

Revised: 3 August 2023

Accepted: 6 August 2023

Published: 30 August 2023



**Copyright:** © 2023 by the authors. Licensee MDPI, Basel, Switzerland. This article is an open access article distributed under the terms and conditions of the Creative Commons Attribution (CC BY) license (<https://creativecommons.org/licenses/by/4.0/>).

## 1. Introduction

The problem of zero-value-cross detection (ZVCD) in single-phase mains-powered motors poses significant challenges for various applications, especially in power tools intended for high-torque tightening operations. Ensuring precise and prompt zero-crossing detection is essential to achieve smooth motor rotation and improve screwing accuracy. This research paper explores different solutions for ZVCD, aiming to reduce delays, simplify complexity, ensure immunity to high voltages, minimize device dimensions, and enhance energy transfer efficiency, which in turn enables the control of higher-power motors.

In the context of ZVCD, minimizing delays in detecting zero-crossing moments is crucial to maintain smooth motor operations. Additionally, the solutions should be robust enough to handle the high voltages typically encountered in single-phase mains-powered motors. To address these challenges, this research examines advanced power semiconductor devices, particularly n-MOSFETs (N-channel metal-oxide-semiconductor field-effect transistors), renowned for their fast switching speed and ability to handle high operation voltages [1]. By utilizing n-MOSFETs, the proposed solutions aim to minimize response times and ensure immunity to high-voltage conditions, improving the reliability and efficiency of the ZVCD system.

In modern power tools, space constraints often demand compact ZVCD solutions without compromising performance. To achieve this, the research focuses on developing compact hardware configurations while maintaining the ability to control higher power motors [2]. This paper investigates various design approaches to achieve these objectives while ensuring compatibility with the single-phase mains-powered motor.

The issue of zero-value-cross detection cannot be disregarded, especially in power tools that rely on single-phase mains-powered motors [1]. The accurate and rapid detection of zero-crossing moments is fundamental to achieving reliable and smooth motor rotation, ensuring the power tool's optimal performance and precision during high-torque tightening

operations. The significance of ZVCD in power tool applications warrants the exploration of novel and effective solutions, which is the primary objective of this research paper.

As the introduction serves as an overview of the research paper, specific details about n-MOSFETs, TRIAC-based circuits, and other solutions will be explored in the following sections and subsections of the paper. These sections will delve into the technical aspects, providing in-depth explanations, analysis, and evaluations of the proposed solutions' performance and benefits.

Among the different solutions being considered for ZVCD, TRIAC-based circuits stand out due to their cost-effectiveness and simplicity. TRIACs provide a viable and practical approach for AC power control, making them suitable for phase control circuits in motor speed regulation. The simplicity of TRIAC-based circuits ensures an ease of implementation and maintenance, while their cost-effectiveness allows for widespread adoption in various applications, including power tools and other consumer electronics. The problem of zero-value-cross detection (ZVCD) is generally well known, as well as its solutions [1,3,4]. Concurrent research tends rather to three-phase brushless motors cooperating with inverters, e.g., [5–7]. However, a specific realization of hardware depends on many factors, like the parameters of the input signal, a type of power supply, and a kind of receiver of zero-cross-moment information. Sometimes, an additional limit adds space available for the hardware.

The authors faced the problem of developing new digital control hardware for a power tool to screw bolts with high torque. The power tool consists of a one-phase mains-powered motor. During the experiments, it became apparent that a reliable and fast cross-detecting signal is crucial for smooth motor rotation and for the improvement of screwing accuracy. Usually, unfortunately, the more accurate and fast one is demanded to be, the more sophisticated the structure is required to be.

This paper presents issues that were encountered during the development of the subcircuit. This paper contains solutions that were taken into account by the authors during the gradual approach to the goal. The behaviors of the electronic circuits presented in this article are calculated with the support of NG Spice [8] and KiCad [9], although all of the presented solutions have been realized and tested in practice. The main contributions of this paper are as follows:

- This paper addresses the problem of zero-value-cross detection (ZVCD) in a single-phase mains-powered motor used in a power tool for screwing bolts with high torque.
- The authors present four different applications for ZVCD, including resistor-polarized digital input, a resistor-polarized optocoupler, comparators steering up the optocoupler, and n-MOSFETs polarizing the optocoupler. Those four are the solutions that are most popular while providing low-cost elements and limited complexity.
- The performance and characteristics of each ZVCD application are analyzed and compared in terms of complexity, dimensions, power dissipation, and response time.
- The n-MOSFET-based solution is identified as the most favorable due to its simplicity, small power dissipation, and almost instant response time, meeting the project's requirements.

We organized the rest of this paper as follows. First, we cover the motivation for research and describe the four most popular solutions in zero cross detection. Then we present the results of the experiments for of the described applications. We then discuss the advantages and limitations of each solution and mention other applications that are not discussed in this paper. We finish with conclusions and a list of considered references.

## 2. Materials and Methods

In this section, we first cover the project that was the motivation for this research, then we discuss the four most popular solutions in zero-cross detection, i.e., resistor-polarized digital input, the resistor-polarized optocoupler, comparators steering up the optocoupler, and n-MOSFETs polarizing the optocoupler, which are then analyzed in the following section.

## 2.1. General Concepts of Project

Since a traditional motor with brushes was needed, the triac [4,10,11] was chosen as the direct control element. In turn, the triac is governed by the microcontroller. The main goal of the project is defined as follow: the applied digital control should ensure better accuracy in screwing the bolts than the existing analog solution.

The main parts of the system, the motor and a high-torque gear, are packed in a typical case, similar to a case for handy drill tools. The hardware should be packed inside the case and the user interface with buttons and a digital display should be placed at the top of the case.

Digital electronics should be galvanically isolated from the mains. Since the beginning, it has been well known that there is not much space for hardware. The awareness that the hardware will require good cooling conditions made the design phase a larger impediment.

The presence of brushes and their related problems, such as extra disturbances, is another obstacle.

## 2.2. Zero-Cross Detectors

Below, in the following subsections, four applications are presented for the zero-cross detection of the mains. The first and second solutions are based on naturally conceived ideas with resistors. The third approach utilizes comparators, and the last solution involves two n-MOSFETs.

### 2.2.1. Resistor Polarizing Digital Input

The simple idea of sensing the AC is to connect it to an input line (e.g., digital) through a resistor [11]. Furthermore, to protect the input against excessive voltage, two diodes are added, respectively, between the 3.3 V and 0 V lines (Figure 1).

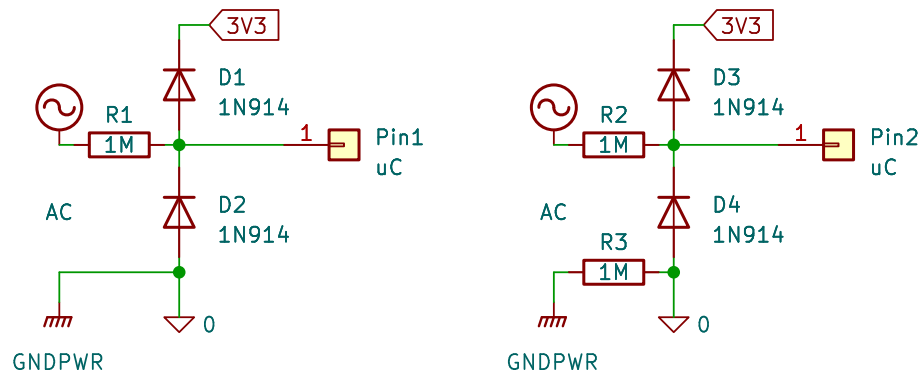


**Figure 1.** Polarization of the microcontroller's input line through a resistor. Basic concept of this detector is presented on the (left) side. The safer version of the circuit is presented on the (right) side (3.3 V has been selected as one of the most popular in recent applications).

On the right side of Figure 1, a safer version of the circuit is presented. The high-value resistor  $R_3$ , connected between the grounded potential and the reference 0 V, among others, protects against the direct influence of the AC high voltage, in the case where the mains is connected in the opposite way.

The diode pairs,  $D_1$  and  $D_2$  and  $D_3$  and  $D_4$ , limit the input voltage of the uC pin in the range  $\approx (-0.7 \text{ V}, 4 \text{ V})$ , when the input voltage changes in the range  $(-325 \text{ V}, 325 \text{ V})$ . The forward current voltage of the diode  $U_{FD} = 0.7 \text{ V}$  is assumed.

In Figures 2 and 3, two simulation models are presented. The first one contains the model of the uC input built with the TTL technique (<https://wiki.analog.com/university/courses/electronics/electronics-lab-27>, accessed on 5 August 2023). The gate has been created with the spice models of the 2N3904 transistor and the 1N914 diode.

In the second scheme (Figure 3), the uC input is simulated as a classic CMOS inverter. The model is based on the MOS transistors in channels n and p: BS250 and 2N7002, respectively. The diodes are again simulated with the 1N914 model.

In both models, the zero-cross detection circuit is the same as the one presented above in Figure 1.

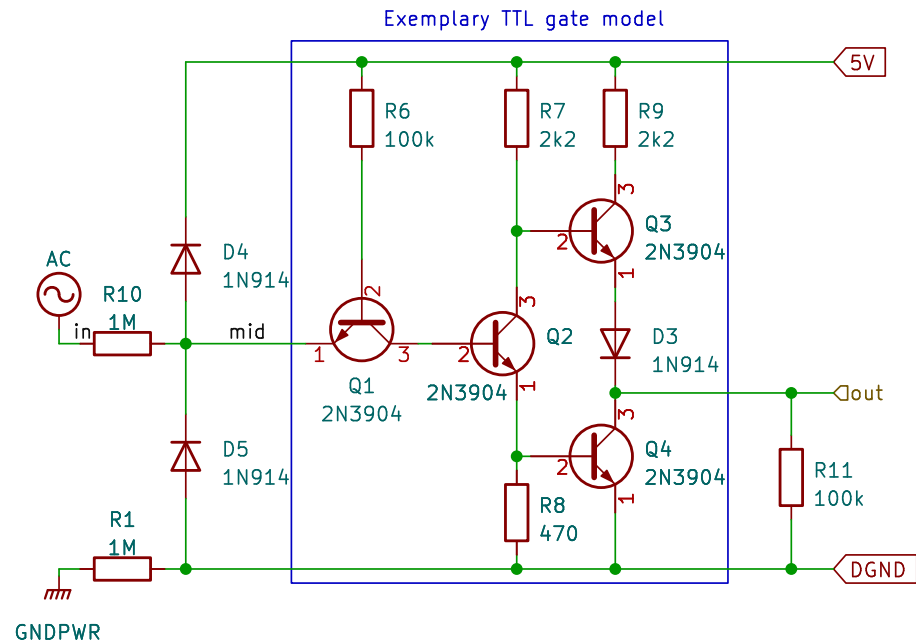


**Figure 2.** ZCVD with the TTL gate simulation model. The TTL gate is modeled discretely, to be able to adjust its specific parameters individually.

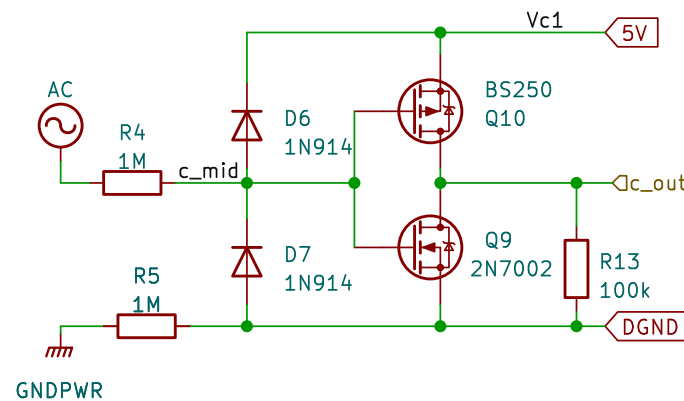


**Figure 3.** ZCVD with the CMOS inverter model. The CMOS inverter is modeled discretely, to be able to adjust its specific parameters individually.

### 2.2.2. Resistor Polarizing Optocoupler

Another way to have a ZVCD signal is to polarize an infrared diode of the optocoupler via a resistor. Figure 4 presents the exemplary scheme. In the negative direction of the mains voltage, the Schottky diode  $D_2$  protects the optocoupler diode against excessive values of the reverse voltage.

Zero-crossing information can be taken directly from the collector (pin #5) of the optocoupler transistor. The isolated part is adjusted to the 3.3 V. The selected optocoupler (CNY17-3 [12]) works properly starting from the 2 mA current flowing through the infrared emitter diode. For the current conditions mentioned above, the current transfer ratio (CTR) parameter of CNY17-3 is approximately equal to 100%.

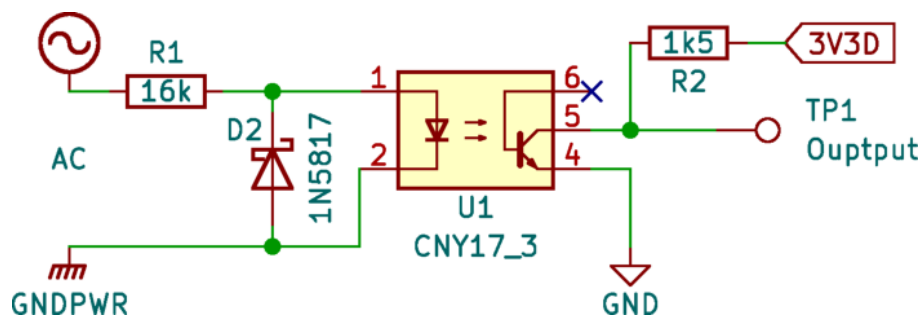


Figure 4. Polarization of the optocoupler through a resistor.

2.2.3. Operational Amplifiers Steering Up Optocoupler

Comparators may be extremely useful in obtaining a digital signal that informs about the crossing of the zero value [1,4]. The exemplary application is presented in Figure 5. In reality, AD8541 is an operational amplifier (op amp), but it can also be used successfully as a comparator [13]. We give relevant parameters of this circuit in Table 1.

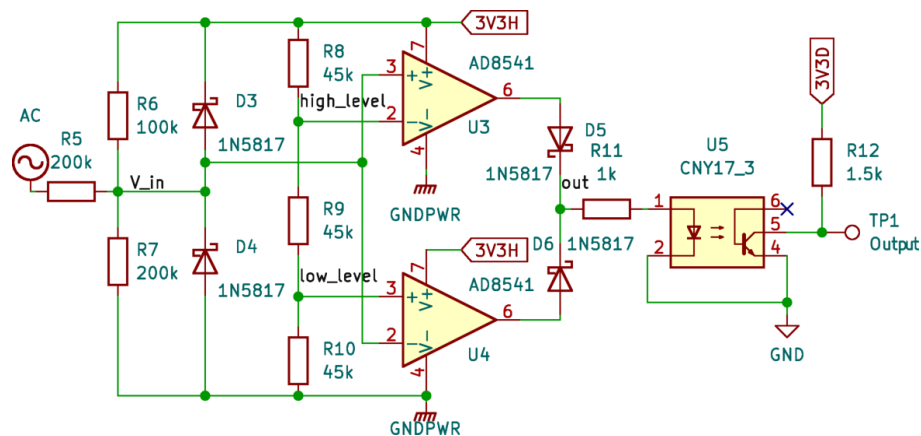


Figure 5. Solution with operational amplifiers and optocouplers.

Table 1. Selected parameters of the AD8544 operational amplifier.

Parameter	Value
Single supply operation	2.7 V to 5.5 V
Input	rail-to-rail type
Output	rail-to-rail

There are two reference values for the voltage setup with resistors R8–R10. The voltage in the pin #3 of  $U_4$  is equal to  $\frac{1}{3}$  of 3.3 V, which is 1.1 V. And the voltage of the pin #2 of  $U_3$  is equal to  $\frac{2}{3}$  of 3.3 V, which is 2.2 V.

When the input voltage is in the range of 1.1–2.2 V, the comparators’ outputs are set to approximately 0 V. When the input voltage is below the minimum value of the above set, the output of  $U_4$  is approximately 3.3 V, and the second comparator output is set to approximately 0 V. When the input voltage is greater than 2.2 V, the comparators’ outputs are set in an inverse way.

Shottky diodes  $D_3$  and  $D_4$  prevent the inputs of the comparators from exceeding the range of their power supply values: 0–3.3 V.

Resistors R6 and R7 initialize the output state of the comparators when no input voltage is received. Shottky diodes  $D_5$  and  $D_6$  realize a simple logic OR gate.

2.2.4. n-MOSFETs Polarizing Optocoupler

Figure 6 presents the ZVCD application that uses n-MOSFET-type transistors to polarize the IRD. The solution involves the LND150 transistors [14] that have a high

value for the maximum drain source voltage,  $V_{DSMax}$  (see Table 2), which makes them capable of connecting directly to the mains. The saturation current,  $I_{DSS}$ , is not too large, but it is sufficient to steer up the optocoupler.

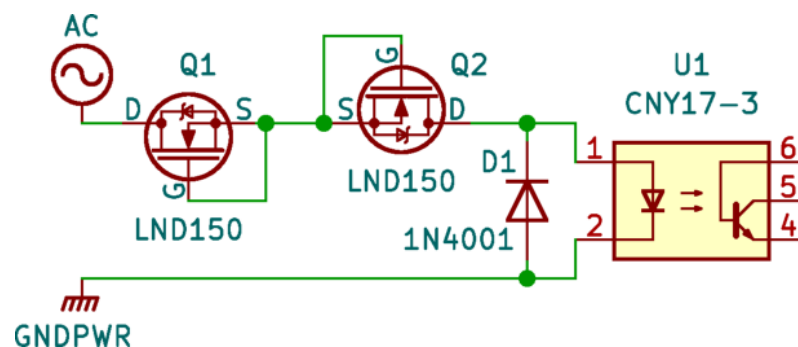


**Figure 6.** The solution with polarization of the optocoupler IR diode by n-MOS depletion-mode transistors. The transistors limit the maximum value of the current, which flows through the IR diode.

**Table 2.** Selected absolute maximum ratings of the LND150 transistor.

Parameter	Value
Drain to source voltage— $V_{DSMax}$	500 V
Drain to gate voltage— $V_{DGMax}$	500 V
Saturated drain to source current— $I_{DSS}$	1–3 mA

When a positive half of the AC sine is applied, a current polarizes the optocoupler through  $Q_1$  and the built-in clamping diode of  $Q_2$ .

When a negative half of the AC sine is applied, a current flows through the protective diode  $D_1$ , the  $Q_2$  transistor, and the built-in clamping diode of the transistor  $Q_1$ . In this case, the optocoupler is not polarized and the diode  $D_1$  protects the IRD of the optocoupler against a break-through voltage (see  $V_{DRMax}$ , Table 3). The  $Q_2$  transistor limits the maximum value of the current to approximately 3 mA (see  $I_{DSS}$ , Table 2), which is similar to  $Q_1$  for the opposite phase of the mains voltage.

**Table 3.** Selected parameters of the CNY17-3 optocoupler.

Parameter	Value
Max. reverse emitter voltage— $V_{DRMax}$	6 V
Max. forward current of the infrared diode— $I_F$	60 mA
Forward voltage for $I_F = 60$ mA— $V_F$	1.39–1.65 V
Isolation test voltage for emitter–detector (1 min)	5000 $V_{RMS}$
Current transfer ratio— $CTR = I_C / I_F$	70–120%

The key for the circuit operation is the saturation current— $I_{DSS}$ —the parameter of the n-MOSFET. The manufacturer's data shows it can vary from 1 to 3 mA and there is no indication of sensitivity to temperature and humidity. Additionally, taking into account it is a digital form of the output, the solution is immune to changes in temperature and humidity in a wide range as well.

### 3. Results

In the following subsections, we present the results of the experiments for the applications described above. Interpretations and conclusions are also added. For the authors, the most important features are as follows:

1. The small dimensions of the solution, which should be placed inside the case of the tool—it is usually also related to a number of electronic elements;

2. Accuracy, the time delay between the moment of the mains crossing 0 V, and the signal informing about that, which should not exceed 100  $\mu\text{s}$ , which stems from the stable control conditions of a microprocessor;
3. A small value of power dissipation, which is desired due to poor cooling conditions inside the case of the tool.

### 3.1. Resistor Polarizing Input of Microcontroller

Figure 7 shows the response of the ZCVDs involving the CMOS and TTL technology (see Figures 2 and 3, respectively).

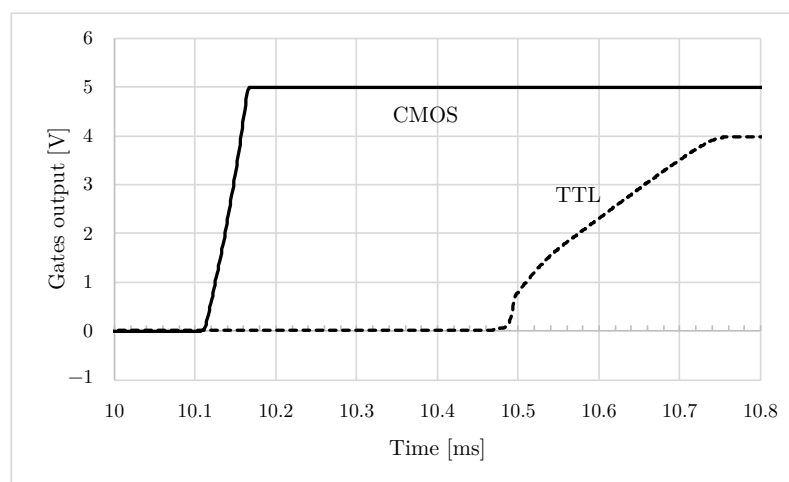


**Figure 7.** Signals at the outputs of the CMOS (solid line) and TTL (dashed line) gates. It can be observed that CMOS is approximately 6 times faster in reaching a high state. TTL does not reach 5 V, because of its structure—the diode D3 in Figure 2 reduces the voltage by approximately 0.7 V.

The horizontal axes represent the time in milliseconds. The ZCVDs are fed with the AC signal, with the period equal to 20 ms. Every 10 ms, the input voltage crosses the zero volts level. The CMOS output sets logic “1” about 160  $\mu\text{s}$  after the crossing moment, and the TTL one reacts near 500  $\mu\text{s}$  and sets the output to logic “1”, approximately 750  $\mu\text{s}$  after the crossing moment.

### 3.2. Resistor Polarizing Optocoupler

Applying the resistor in a circuit that polarizes the optocoupler is the simplest and most popular solution (see Figure 4). As the maximum value of  $I_{Fmax}$  (see Table 3) is equal to 60 mA, the infrared diode current  $I_F = 20$  mA was selected as a safe and fairly good point of work. The mains voltage changes approximately in the range of  $-325$  V to 325 V, so the resistor was designed so that the current flowing in the circuit does not exceed 20 mA at the maximum value of the mains, which is equivalent to the resistance equal to 16 k $\Omega$ . Figure 8 presents the SPICE simulation results for the above situation.

The tests and data sheets suggest that CNY17-3 begins working confidently with current  $I_F \approx 2$  mA. In the application, it occurs after about 335  $\mu\text{s}$  from the moment the mains crosses 0 V, when  $V_{mains} \approx 34$  V (see Figure 9).

The delay may be reduced by decreasing the resistance. Knowing that the maximum current value for the IRD is equal to 60 mA, the minimum resistance that can be set is 5.4 k $\Omega$ . The change decreases the time delay to the new value: 0.11 ms. The new, better value of the delay costs an increasing power consumption, which is equal to 9.8 W now! In Figure 10, it is updated.

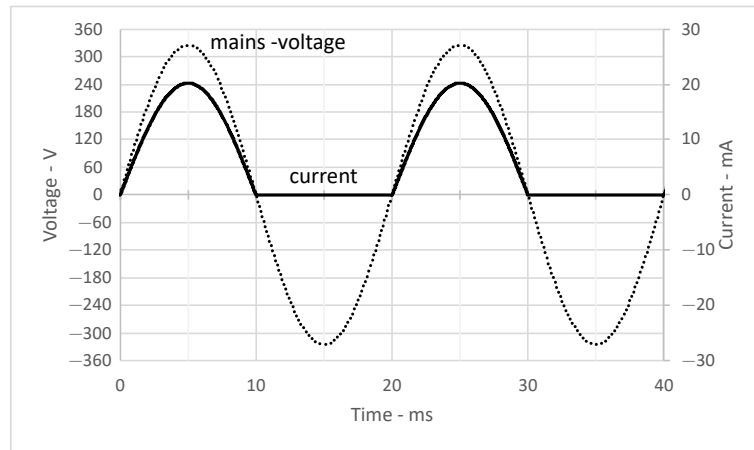


**Figure 8.** Comparison of mains voltage and current flowing through the resistor and the IRD optocoupler circuit. It can be observed that the current is linearly dependent on the circuit (in the positive semi period) and cannot be faster than the voltage.

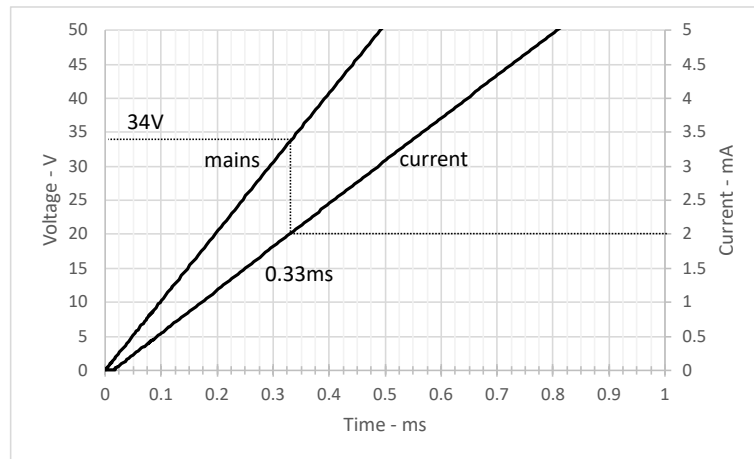


**Figure 9.** Magnification of Figure 8 in a range of 0 to 1 ms of current flowing through the resistor and IRD circuit and corresponding mains voltage. It can be observed that the recommended current is reached after 335  $\mu$ s at a voltage of 34 V.

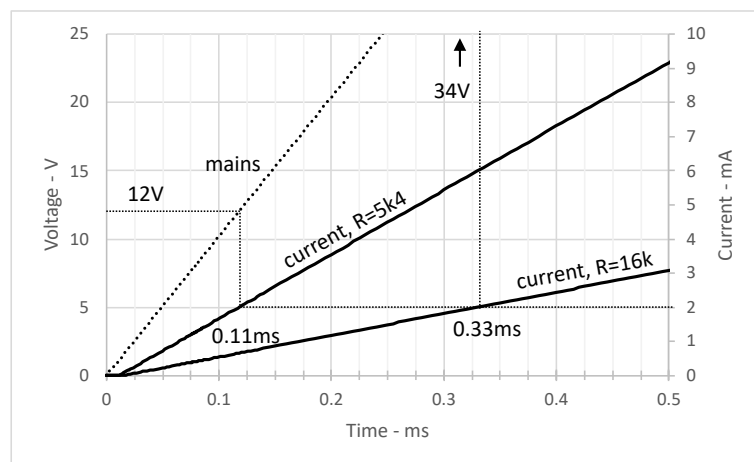


**Figure 10.** Current flowing through the resistor and IRD for two resistance values, scaled in the range of 0 to 0.5 ms. It can be observed that change in resistance can reduce the time to reach the recommended current to  $\approx$ 11 ms at the cost of power consumption.

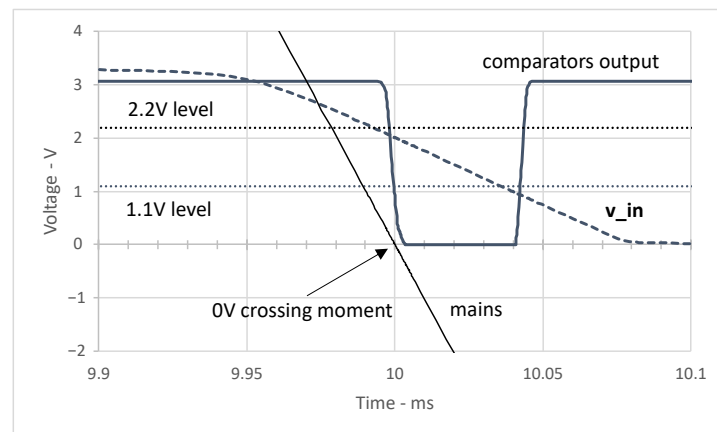
### 3.3. Operational Amplifiers Steering Up Optocouplers

Figure 11 shows the selected signals of the ZVCD based on the amplifiers while the mains is crossing 0 V. When the input voltage:  $v_{in}$  (see Figure 5, junction of R5–R7) is between low and high levels, both comparators set their output to 0 V, which, in consequence, sets the output signal to 0 V (see Figure 5 for the junction of elements D5, D6, and R11, along with the dashed line in Figure 11).

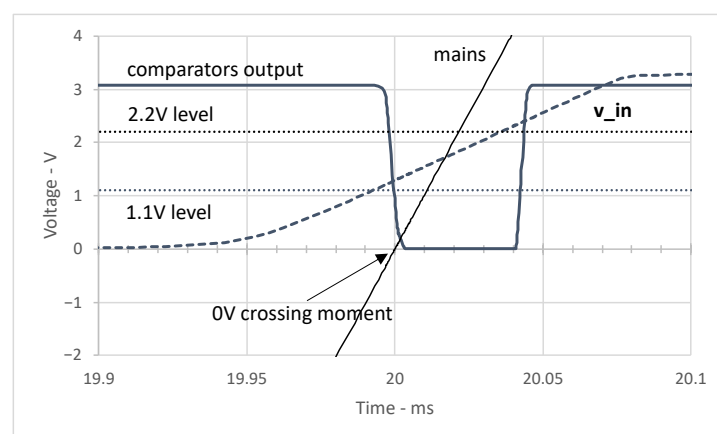
When  $v_{in}$  leaves the interval 1.1–2.2 V, the output increases to a high level. The transition time of the output signal is  $\approx 5 \mu\text{s}$ . The width of the output signal is  $\approx 40 \mu\text{s}$ , which may be set in certain limits by the resistor relations R8–R10.

Figure 12 presents the reaction of the circuit when the mains crosses the point 0 V as the voltage increases. The situation is analogous to the previous one. The moment of crossing 0 V is signaled by the zero pulse, which has a width similarly equal to  $\approx 40 \mu\text{s}$ .

The circuit reactions in both cases are almost instant with a tolerance of a slope duration, which is  $\approx \pm 2.5 \mu\text{s}$ .



**Figure 11.** Response of the circuit with operational amplifiers (see Figure 5) at the 0 V mains crossing with negative slope (falling voltage). We can see that the comparator output drops below the 1.1 V level (indistinguishable from 0 V for the microcontroller) immediately, i.e., a few  $\mu\text{s}$ , when the mains' 0 V crossing occurs.



**Figure 12.** Response of the circuit with operational amplifiers (see Figure 5) at the 0 V mains crossing with positive slope (rising voltage). We can see that, as in the case of negative slope, the comparator output drops below the 1.1 V level (indistinguishable from 0 V for the microcontroller) immediately, i.e., a few  $\mu\text{s}$ , when the mains' 0 V crossing occurs.

### 3.4. n-MOSFETs Polarizing Optocoupler

When the AC voltage drops and approaches  $\approx 3 \text{ V}$ , the n-MOSFET goes out of saturation ( $I_{DSS} \approx 2.3 \text{ mA}$ ) and its current starts decreasing to 0 A (see Figure 13). The current

stops flowing when the mains voltage is about 1 V, which is derived from the value  $V_F$  (see Table 3), so the signal informing about the zero crossing of the mains is made in advance,  $\approx 10 \mu\text{s}$ .

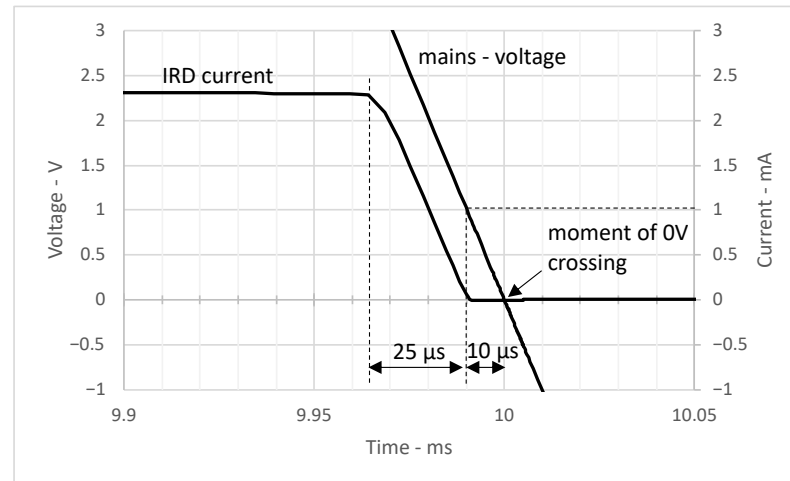


**Figure 13.** Response of the n-MOSFET depletion-type transistor circuit (Figure 6) at the 0 V mains crossing with negative slope (falling voltage). We can see that the IRD current, i.e., detection signal, drops to zero  $10 \mu\text{s}$  before the actual mains 0 V crossing.

An analog situation occurs when the mains voltage increases (see Figure 14), but this time the signal that informs about the crossing of 0 V is late by  $\approx 35 \mu\text{s}$ ; again, the IRD current starts flowing when the mains voltage is at least equal to 1 V.

The time of the current transition is  $\approx 25 \mu\text{s}$  in both cases.

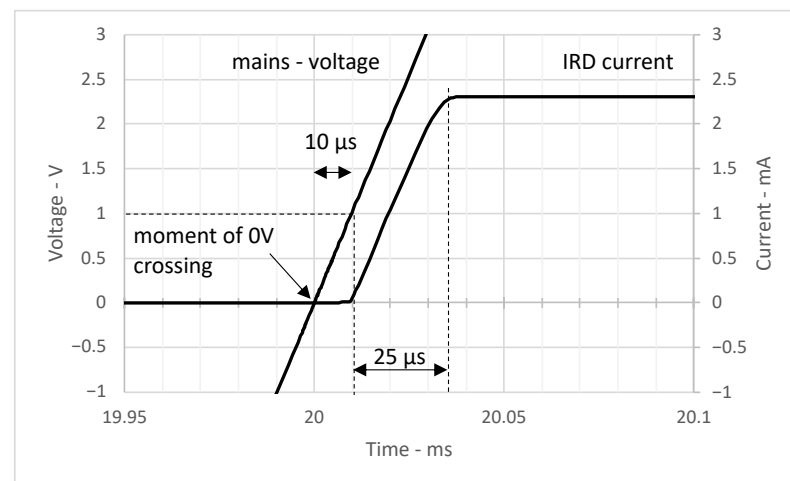


**Figure 14.** Response of the n-MOSFET depletion-type transistor circuit (Figure 6) at the 0 V mains crossing with positive slope (rising voltage). We can see that the IRD current, i.e., detection signal, starts flowing  $35 \mu\text{s}$  after the actual mains 0 V crossing.

#### 4. Discussion

It should be mentioned that all analyzed solutions can be used in motors of different ratings, as they are not included in the power electronics part of the controller.

##### 4.1. Resistor and Microcontroller

The results show an apparent advantage of the CMOS over the TTL solution. The CMOS application in the ZCVD results in a response about six times faster.

The delay, greater than half a millisecond in the response of the TTL gate, is due to parasite capacitors of bipolar transistors and favors a high  $1 \text{ M}\Omega$  resistance of protective

resistors  $R_1$  and  $R_{10}$  (see Figure 2). The delay may be decreased by using resistors with a lower resistance; however, it follows that there would be a worsening protection against the AC influence.

#### 4.2. Resistor and Optocoupler

The advantage of resistor polarization is simplicity. Only two elements are needed: the resistor and the protective diode. However, the power the resistor dissipates is equal to 3.3 W, leading to larger dimensions and a worsening of the cooling conditions in the tool case. Furthermore, the delay equal to  $\approx 0.3$  ms is bigger than the assumptions of the project.

The new value of the delay response for the smaller resistor is equal to 0.11 ms and is much better than the previous one, but, as a consequence, the power consumption increases to 9.8 W (see Figure 10).

#### 4.3. Operational Amplifiers

An amplifier-based solution requires an additional DC power supply, which may be a serious impediment, but, in exchange for it, a response of the electronic system is almost instant. Particularly, the answer may be set up in advance by appropriately selected input resistors and levels of reaction by the comparators.

#### 4.4. n-MOSFET

Transistors in the application ensure that there is no excess of the safe value of the IRD current, although the mains voltage varies in the range ( $-325$  V,  $+325$  V). The current increases to the maximum value in 25  $\mu$ s, which is derived from the main frequency and the output characteristics of the transistor (drain current vs. voltage across the drain source;  $I_D = f(U_{DS})$ ). The application consists only of two transistors and one Shottky diode.

There is no need for an additional power supply, and the power dissipation by the single transistor is small:  $P_{tran} = 1/2 \cdot 230$  V  $\cdot$  2.3 mA  $\approx$  0.26 W. The power dissipation by the diodes, IRD, Shottky, and built-in, is in the order of milliwatts and may be neglected. The minimal reaction time of the application is equal to  $\approx 10$   $\mu$ s and is derived from the  $V_F$  of the IRD (see Table 3). The transition time of the current is  $\approx 25$   $\mu$ s, so the reaction time of the solution is in the range ( $-10$   $\mu$ s,  $+35$   $\mu$ s) when the mains voltage drops and increases, respectively.

#### 4.5. Optocoupler Delay

As it is a common case for all solutions and an optocoupler delay is an individual characteristic, it has not been discussed separately. However, to have a complete view of the problem, in Figure 15 the delay in the optocoupler response in the circuit with the comparators is presented.

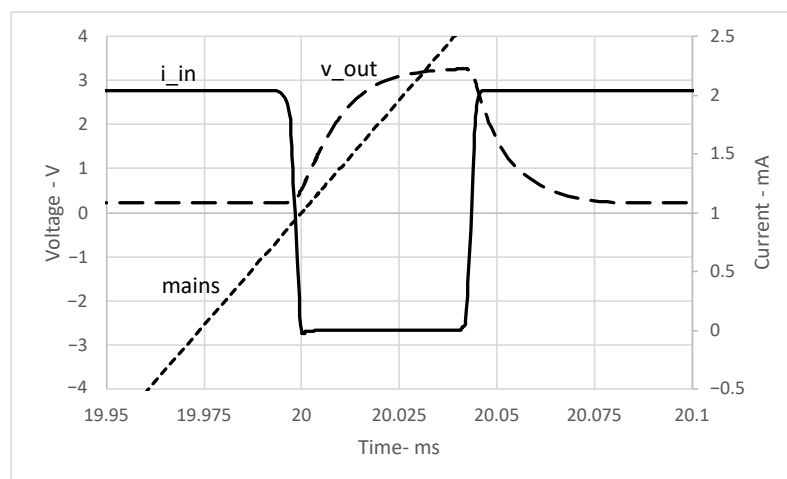


Figure 15. Optocoupler delay.

It is easy to notice the delay because the action of the comparators is very fast with reference to the optocoupler delay. The current of the IRD is represented as  $i_{in}$  and the output voltage of the optocoupler is marked as  $v_{out}$ . The voltage  $v_{out}$  approaches the 3.3 V level after  $\approx 25 \mu\text{s}$ . See also Figure 5— $v_{in}$  corresponds to the current flowing into pin #1 of CNY17-3 and  $v_{out}$  to pin #5 of CNY17-3.

#### 4.6. Technical Limitations

All the investigated solutions have their practical limitations. Using a microcontroller with a resistor comes from minimal reaction levels of either TTL or CMOS. This causes unavoidable delays. A solution based on a resistor and optocoupler allows a reduction in delays but at large costs of power. Operational amplifiers, while definitely the fastest solution, require the most sophisticated circuit that requires more space on the board. Finally, n-MOSFET circuits have unavoidable delays regardless of parameter modification; however, they were still our preferred solution.

#### 4.7. Not Analyzed Solutions

In this paper, we have not exhausted all possible realizations of ZVCD. The following are examples:

- An integrated sensor with a very fast A/D converter measuring the mains voltage;
- A dedicated ASIC circuit integrating all things on the chip;
- A circuit for a dual-point interpolation method for detecting a zero crossing (see [3]).

They were not considered because of specific reasons. The goal was a very small in size and low in cost solution that will ensure required time regimes. A fully digital solution increases the load on the entire digital control system and can become size-prohibitive. ASICs are totally cost-prohibitive. And a solution with dual-point interpolation requires two optocouplers, which would exceed size constraints.

## 5. Conclusions

The following categories were taken into account when solving the problem: complexity, dimensions, power dissipation, and quality. The applications of two “resistors” have bigger dimensions and are first of all slow. Moreover, the second version also dissipates a lot of power.

The solution based on operational amplifiers has the best quality but requires an extra power supply and many elements for realization, which lead to a demand for higher dimensions as well. The last one, which uses n-MOSFETs, does not need an additional power supply and consists of only three elements. The power dissipation is also small. The quality is not as perfect as that achieved with operational amplifiers; however, the delay of tens of microseconds is fully acceptable for our goal. Additionally, the n-MOSFET is a very cost-effective solution. In particular, its cost compares to standard discrete electronic elements.

Table 4 presents a brief summary of the above, in numbers, and Figure 16 shows graphically the comparison of the IRD current, on the same scale, for both solutions: the resistor and MOSFETs.

**Table 4.** Summary of the solutions. A negative value of the delay means “in advance”.

Solution	Complexity	Dimensions	Power Dissipation	Quality	Delay
Resistor and microcontroller	a few elements	medium	small	poor	160 $\mu\text{s}$
Resistor and optocoupler	2 elements	big	big, even 10 W	poor	335 $\mu\text{s}$
Operational amplifiers	many elements and additional power supply	big	medium	very high	(2 $\mu\text{s}$ , 3 $\mu\text{s}$ )
n-MOSFETs		small	medium	medium	(−10 $\mu\text{s}$ , 35 $\mu\text{s}$ )

A key limitation of our study is the fact that it considers TRIAC control. In case of, e.g., inverter solutions, the considered time regimes can be too long. We have observed that the

motor works much more fluently, so it is expected that the lifespan will be extended and work will be more efficient. Further research will verify that hypothesis.

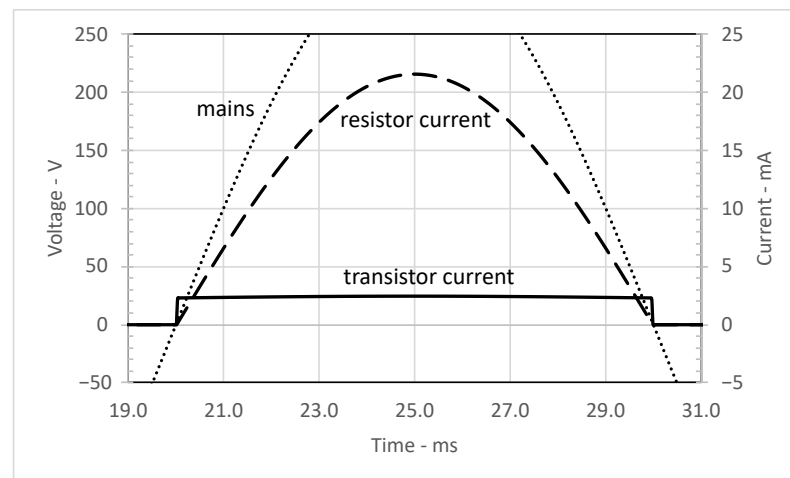


**Figure 16.** Comparison of two solutions: resistor versus transistor polarizing optocoupler.

**Author Contributions:** Conceptualization: M.P. and P.P.; formal analysis: M.P., P.P. and J.B.; funding acquisition: P.P. and J.B.; investigation: M.P. and P.P.; methodology: M.P. and P.P.; project administration: P.P.; resources: M.P. and P.P.; software: M.P.; supervision: P.P.; validation: M.P. and P.P.; writing—original draft: M.P.; writing—review and editing M.P., P.P. and J.B. All authors have read and agreed to the published version of the manuscript.

**Funding:** This work was partially funded from the project titled “Smart Electric Torque Tool”, which was financed by the National Centre for Science and Development under contract no. INNOTECH-K3/48/225932/NCBR/14 and partially from AGH University of Krakow subvention for scientific activity no. 16.16.120.773.

**Institutional Review Board Statement:** Not applicable.

**Informed Consent Statement:** Not applicable.

**Data Availability Statement:** The data presented in this study are available on request from the corresponding authors.

**Acknowledgments:** We would like to thank Tomasz Dziwiński for his help.

**Conflicts of Interest:** The authors declare no conflicts of interest.

## Abbreviations

The following abbreviations are used in this manuscript:

AC	Alternating current
ASIC	Application-specific integrated circuit
CTR	Current transfer ratio
uC	Microcontroller
DC	Direct current
DOAJ	Directory of Open-Access Journals
IR	Infrared
IRD	Infrared diode
MDPI	Multidisciplinary Digital Publishing Institute
MOSFET	Metal-oxide-semiconductor field-effect transistor
OPA	Operational amplifier
RMS	Root mean square
SPICE	Simulation Program with Integrated Circuits Emphasis
ZVCD	Zero-value-cross detector

## References

1. Horowitz, P.; Hill, W. *The Art of Electronics*, 3rd ed.; Cambridge University Press: New York, NY, USA, 2015.
2. Wall, J. Power Conversion for IoT Devices: A Comprehensive Review. *IEEE Trans. Power Electron.* **2019**, *22*, 45–56.
3. Wall, R.W. Simple methods for detecting zero crossing. In Proceedings of the IECON'03, the 29th Annual Conference of the IEEE Industrial Electronics Society (IEEE Cat. No.03CH37468), Roanoke, VA, USA, 2–6 November 2003; Volume 3, pp. 2477–2481. [[CrossRef](#)]
4. Philips Semiconductors. Philips 51LPC-Microcontrollers & Triacs Easily Connected. Application Note 467\_1. 2000. Available online: <https://www.datasheetarchive.com> (accessed on 16 May 2023)
5. Ahmad, F.; Pandey, M.; Zaid, M. Sensorless Control of Brushless DC Motor by Zero-Crossing Detection Pulse Generation with Adaptive Power Factor Control Technique. In Proceedings of the 2018 IEEE International Conference on Environment and Electrical Engineering and 2018 IEEE Industrial and Commercial Power Systems Europe (EEEIC/I&CPS Europe), Palermo, Italy, 12–15 June 2018; pp. 1–6. [[CrossRef](#)]
6. Patil, T.; Ghorai, S. Robust zero-crossing detection of distorted line voltage using line fitting. In Proceedings of the 2016 International Conference on Electrical, Electronics, Communication, Computer and Optimization Techniques (ICEECCOT), Mysuru, India, 9–10 December 2016; pp. 92–96. [[CrossRef](#)]
7. Yu, J.; Wen, Y.; Yang, L.; Zhao, Z.; Guo, Y.; Guo, X. Monitoring on triboelectric nanogenerator and deep learning method. *Nano Energy* **2022**, *92*, 106698. [[CrossRef](#)]
8. Ngspice, the Open Source Spice Circuit Simulator—Intro. Available online: <https://www.ngspice.sourceforge.io> (accessed on 17 April 2023).
9. KiCad EDA—A Cross Platform and Open Source Electronics Design Automation Suite. Available online: <https://www.kicad.org> (accessed on 17 April 2023).
10. Philips Semiconductors . Power Semiconductor Applications. Available online: <https://scholar.google.com> (accessed on 16 May 2023).
11. STMicroelectronics. Universal Motor Speed Control and Light Dimmer with TRIAC and ST7LITE Microcontroller. Application Note, AN 2263. Available online: <https://www.datasheetarchive.com/> (accessed on 16 May 2023).
12. Vishay Co. CNY17-3. Available online: <https://www.vishay.com/docs/83606/cny17.pdf> (accessed on 7 March 2023).
13. Analog Devices Co. ad8541/ad8542/ad8544 General Purpose CMOS Rail-to-Rail Amplifiers Data Sheet (Rev G). Available online: <https://www.analog.com/en/products/ad8544.html#product-reference> (accessed on 7 March 2023).
14. Microchip Technology. LND150. Available online: <https://www.microchip.com/en-us/product/LND150> (accessed on 7 March 2023).

**Disclaimer/Publisher’s Note:** The statements, opinions and data contained in all publications are solely those of the individual author(s) and contributor(s) and not of MDPI and/or the editor(s). MDPI and/or the editor(s) disclaim responsibility for any injury to people or property resulting from any ideas, methods, instructions or products referred to in the content.